Automated parametric Rietveld refinement: Applications in reaction kinetics and in the extraction of microstructural information

P. Rajiv, R. E. Dinnebier,[a] and M. Jansen
Max Planck Institute for Solid State Research, Heisenbergstraße 1, 70569, Stuttgart, Germany

M. Joswig
Institute for Geophysics, Stuttgart University, Azenbergstraße 16, 70174, Stuttgart, Germany

(Received 4 August 2011; accepted 11 October 2011)

Two applications of parametric Rietveld refinement employing a newly developed robust computer program are presented. The first application focuses on the parametric kinetic analysis of the reactions involving phase transitions of various polymorphic forms of copper phthalocyanine pigments. The second application concerns the parameterization of crystallite size with respect to experimental temperature. XRPD data for nanocrystalline titanium dioxide measured in dependence on temperature are used in this case study. Both the applications were realized with the help of the developed program in combination with the launch mode of TOPAS® software. © *2011 International Centre for Diffraction Data*. [DOI: 10.1154/1.3662220]

Key words: parametric Rietveld refinement, sequential Rietveld refinement, crystallite size, reaction kinetics, copper phthalocyanine, titanium dioxide, TOPAS

I. INTRODUCTION

Parametric Rietveld refinement (Stinton and Evans, 2007) is a robust method for acquiring physical/chemical information of materials studied using 2D XRPD. A newly developed computer program "POWDER 3D PARAMETRIC" (Rajiv *et al*., 2010), in combination with the TOPAS® launch mode (Coelho, 2007), has recently been introduced to perform fast sequential and parametric whole powder pattern fits (WPPF) of large number of powder patterns collected in 2D XRPD experiments. This paper presents a general demonstration of sequential and parametric WPPF performed using "POWDER 3D PARAMETRIC," followed by two applications of parametric Rietveld refinement that were accomplished with the help of the developed program.

The demonstration of sequential/parametric WPPF performed using "POWDER 3D PARAMETRIC" is presented in Sec. III of the paper. The sample used in this demonstration is copper phthalocyanine (Cu*PC*) XRPD data (Müller *et al*., 2010) measured in a time-dependent manner (isothermal data) at a synchrotron source. This sample is one among several time-dependent data of Cu*PC* polymorphs and Cu*PC* polymorph-additive mixtures (Table II) that were measured with the objective of studying their reactions kinetics using the parametric Rietveld refinement method. In such time-dependent experiments, the simultaneously varying weight fractions of the polymorphs with time contain the reaction kinetic information (e.g., the reaction rate constant k). These information were extracted during the multiphase Rietveld analysis, by parameterizing the weight fractions (Hill and Howard, 1987) of one of the phases of the polymorphic Cu*PC* [as explained in Müller *et al*. (2010)] with the well known Avrami equation, a function of reaction rate constant k and a constant n (Avrami, 1939; Avrami, 1941; Farjas and Roura, 2006; Malek and Mitsuhashi, 2000). The set of rate constants (Table II), derived from the Avrami model at various temperatures can be used to determine the activation energies of the reactions. The summary of kinetic analysis performed using parametric Rietveld refinement on several Cu*PC* data measured in dependence on time is provided in Sec. IV.

Similar analyses on Cu*PC* were formerly performed by M. Müller *et al*. (2010), in which the reaction kinetic information (k) of Cu*PC* polymorphs was extracted using the full quantitative sequential Rietveld analysis and an Arrhenius type of relation (Iordanova *et al*., 2002). In this paper, the rate constants (k) obtained from the literature (Müller *et al*., 2010) and those derived from the Avrami model are compared; the discrepancies between the two results are briefly discussed.

The final part of the paper (Sec. V) presents a basic demonstration of the parameterization of the crystallite size variation with respect to the annealing time/temperature. The temperature dependent nanocrystalline titanium dioxide (TiO_2) data are used as examples. The variation of the crystallite size (inversely related to the FWHM of the phase peaks) with respect to temperature for some selected data samples could be parameterized by a general third order polynomial.

II. THE PROGRAM

All the refinements required for the two applications were performed in the launch mode of the TOPAS software, where the set of instructions necessary to perform a WPPF is entered in a text file (input or *.*inp* file) and passed to the TOPAS kernel for execution.

The kinetic analysis of Cu*PC* required about 19 independent isothermal data to be treated with sequential and parametric Rietveld refinements (Table II); each data consists of an average of about 140 powder patterns measured at various fixed temperatures. The parameterization of the crystallite size of TiO_2 required 90 temperature-dependent powder patterns to be refined sequentially and parametrically. This analysis also required several models of crystallite size to be tested before arriving at the optimal.

[a]Electronic mail: r.dinnebier@fkf.mpg.de

The flexible macro language of TOPAS can be used in several ways to conveniently modify an existing variable or to introduce a model of the existing variable or to introduce a new variable etc., during the refinement. However, manual modification of the TOPAS statements, and the preparation (and execution) of the input files, and manual organization of the refined output variables for the analyses involving numerous powder patterns (as in the present case) is a monotonous and time consuming task. The program "POWDER 3D PARAMETRIC" has therefore been used in the preparation and execution of all the input files used in the sequential and parametric refinements and also in some graphical presentations related to the two applications. The program offers a GUI platform for quicker and easier preparation and execution of the input files and also supports parametric refinements involving several trials with different variable models used in each trial (as in the case of the crystallite size analysis, Sec. V). The program uses the TOPAS launch mode only as a kernel where the "math" parts of the refinements are performed.

III. A CASE STUDY

In this section, the WPPF of a single powder pattern (denoted "test" WPPF/refinement), the sequential refinements, and the parametric refinement in relation to the isothermal kinetic analysis of Cu*PC* performed using the program are demonstrated. The procedure for the sequential refinements associated with the crystallite size analysis is the same as that described in this section. (For the "parametric crystallite size" analysis, the required input files were prepared using the program, but the prepared files are executed in the TOPAS GUI mode.)

The sample used in this case study (denoted test-sample) is a mixture containing the α and β phases of Cu*PC* in the ratio of 9:1 at the onset of the experiment. The experiment was performed in dependence on time at a constant temperature of 270 °C. In total, 35 powder patterns were collected in this experiment.

A. A single refinement

Prior to the sequential/parametric refinements, POWDER 3D PARAMETRIC obliges the user to perform the test refinement of a single powder pattern in the data. The pattern used in the test refinement is usually the one measured at the lowest time step (or temperature) or the pattern from which the user wishes to begin the sequential refinements.

The input file required to refine the test pattern can be built using the text editor interface provided by the program (Figure 1). Some of the TOPAS macro commands and the keywords that make up the input file can be conveniently loaded into the editor with the help of various widget tools supplied by the program. (Alternatively, a previously prepared input file can be copied/loaded to the text editor.)

After loading the required TOPAS commands into the text editor, the test refinement can be started by prompting the appropriate key provided by the text editor GUI of the program. The results of the test refinement (the convergence plot and the refined variables) will be gathered from the output file ("test.*out*") returned by TOPAS kernel and will be displayed in a separate interface. The user is allowed to inspect and modify the variable values and their refinement flags and repeat the test refinement until acceptable convergence is reached. After attaining a satisfactory convergence, the user is prompted by the program to store the "test.*out*" file.

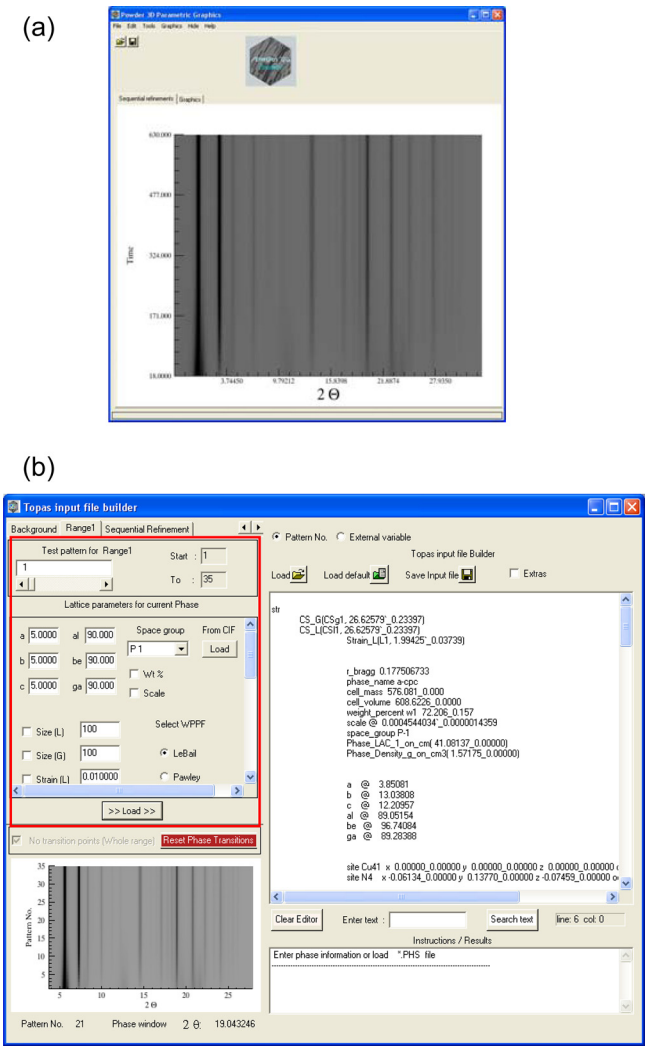

Figure 1. (Color online) (a) The time-dependent simulated "heating Guinier film" plot of the test-sample loaded in the main graphics window is presented (Hinrichsen *et al.*, 2006). (b) The editor interface used for building TOPAS "*.inp" file is shown. The plain text editor is at the right; widget tools used for loading the TOPAS keywords into the editor are highlighted at the left by a rectangular frame.

B. Sequential refinement

Before starting the sequential refinements, all the variables refined in the test refinement are gathered from the stored output file and listed in an interface [Figure 2(a)]. The user must check the variable names, their scopes, and their refinement flag statuses to be used in the sequential refinements. This interface also provides an option to store the sequentially refined variables and their errors in the form of a table, which can be analyzed later using the existing commercial worksheets.

Once the variable names are confirmed and their scopes and their refinement flags are set, the program automatically prepares and executes the input files required for the subsequent refinements of all the powder patterns.

https://doi.org/10.1154/1.3662220 Published online by Cambridge University Press

(a)

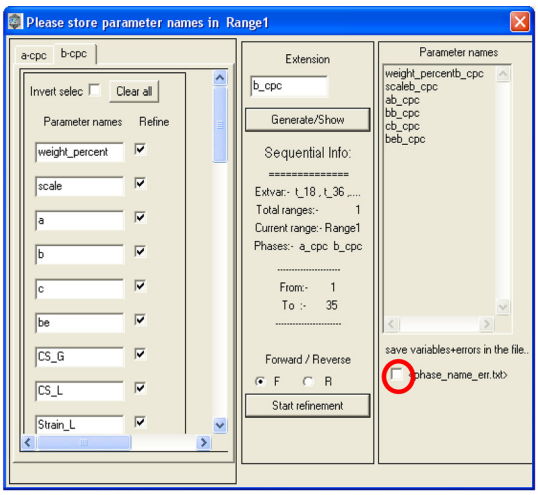

(b)

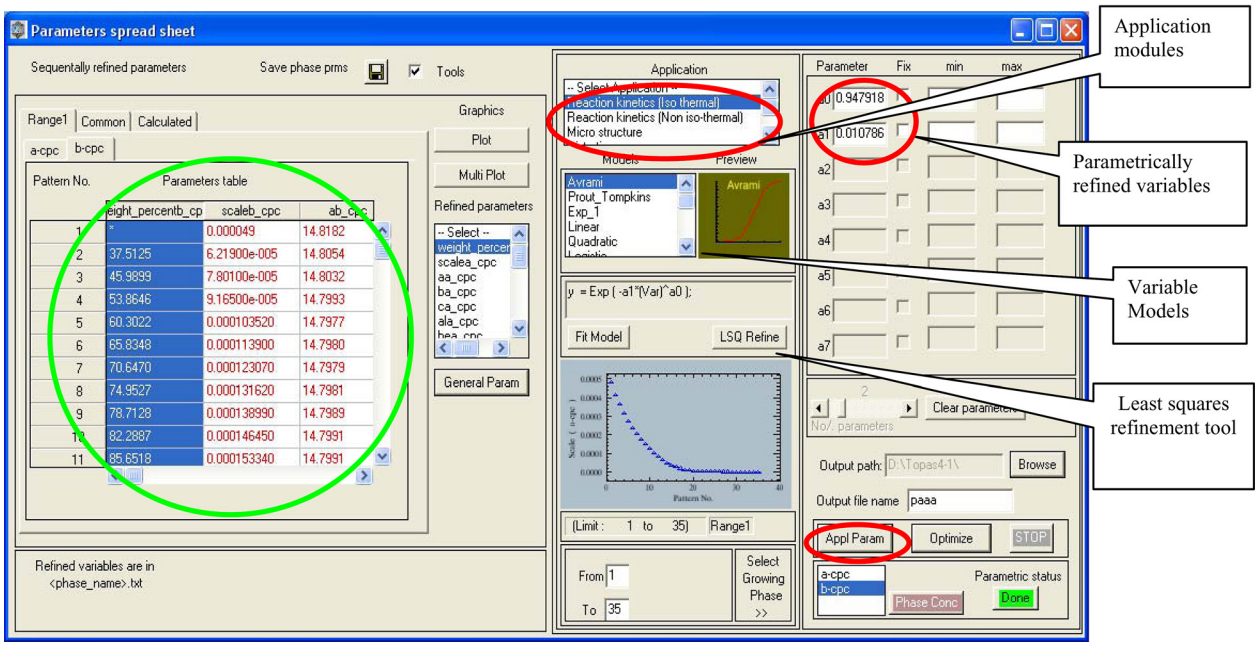

Figure 2. (Color online) (a) "Variable name/flag" interface. The dark circle at the bottom indicates the option to store the refined variables and errors as a table. (b) Some important functions of the "parameters worksheet" are explained in detail. The tools that are relevant to the presented paper are highlighted with circles. The variables obtained in sequential refinements are displayed in the left part of the worksheet (circle).

At the end of all the refinements, the variables refined in each cycle (which were saved beforehand as text files) will be read, sorted, and loaded in a worksheet as in Figure 2(b) (denoted "parameters worksheet"). All the refined variables loaded in the "parameters worksheet" [Figure 2(b)] can be plotted or parameterized by any suitable model provided by the program or by any user-defined functions.

The variables of interest for the reaction kinetics analysis are the weight fractions of the α-β-Cu*PC* phases; these parameters are simultaneously plotted against the time axis at the end of the refinements [Figure 3(a)]. The weighted residuals (r_wp) of the consecutive refinements can also be plotted optionally [Figure 3(b)], which helps the user to select only the data measured within a particular time span to be used in parametric refinement.

C. Parametric refinement

Parametric Rietveld refinement associated with kinetic analysis can be started after selecting the module "*Reaction kinetics-Iso thermal*" and an appropriate model (*Avrami*) from their respective lists provided in the "parameters worksheet" [Figure 2(b)]. The program both prepares and executes the input file (denoted "parametric input file") containing the set of instructions needed to perform parametric Rietveld refinement.

The TOPAS "input file" necessary for the refinement of a single powder pattern consists of two parts (Stinton and Evans, 2007): The first part contains the statements that are common to all the measured patterns (e.g., wavelength, instrumental parameters, Lorentz-polarization factor, convolution step, etc.). The second part (denoted "phase" part) contains the statements that are specific to the measured powder pattern or a particular phase of the compound, if the

https://doi.org/10.1154/1.3662220 Published online by Cambridge University Press

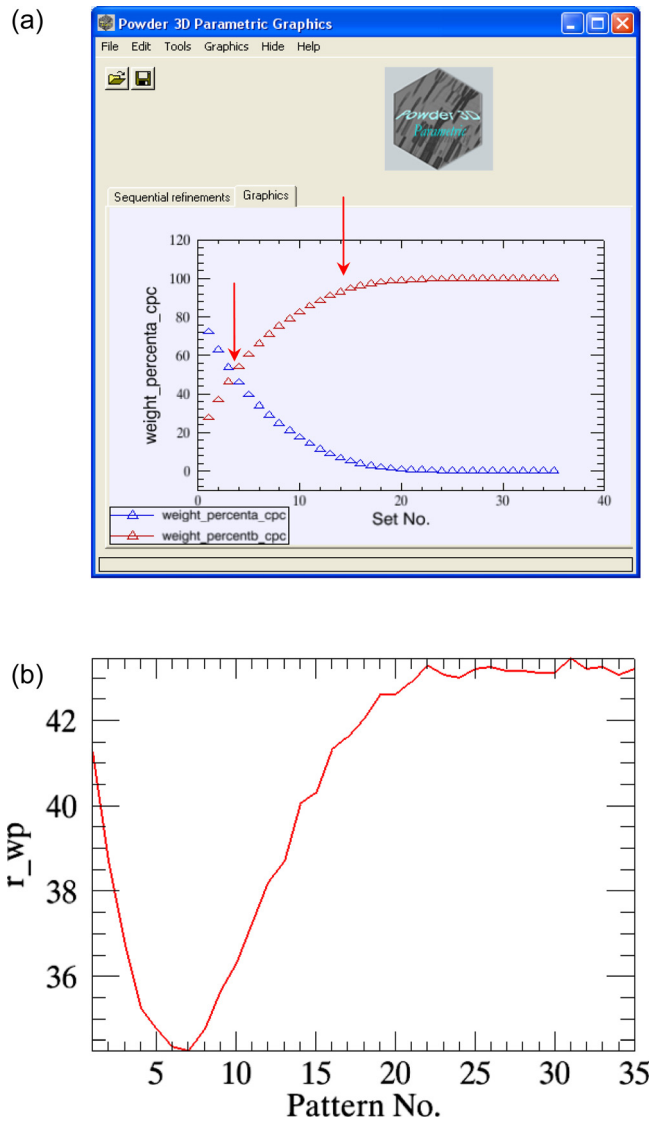

Figure 3. (Color online) (a) The sequentially refined weight fractions of the decaying α-Cu*PC* and the growing β-Cu*PC* of the test-sample are plotted in the "graphics interface". (b) The weighted residuals r_wp (scaled by a factor of 80) of the sequential refinements are plotted.

compound is a mixture. (e.g., the lattice parameters, crystallite size, scale factor, weight fraction, etc.).

For performing multiphase Rietveld refinement of a single powder pattern, the "phase" part of the input file must contain the TOPAS keyword "*scale*," which encodes a rewritten form of Eq. (1) (Hill and Howard, 1987). During refinement, the "*scale*" keyword conveys to the TOPAS kernel that the scale factor of a given phase of the compound containing m phases must be calculated from

$$x_\alpha = \frac{S_\alpha * M_\alpha * V_\alpha}{\sum_{i=1}^{m} (S_i * M_i * V_i)}, \qquad (1)$$

where x_α is the weight fraction of a phase α in a mixture of m phases, which can be parameterized by the Avrami equation: $(1 - \exp(-(kt)^n))$, with k as the reaction rate constant and n as Avrami constant. "t" is experimental time, $(S, M, V)_{\alpha,\beta,\gamma}$ are the scale factors, unit-cell masses, and unit-cell volumes of the phases α, β, and γ.

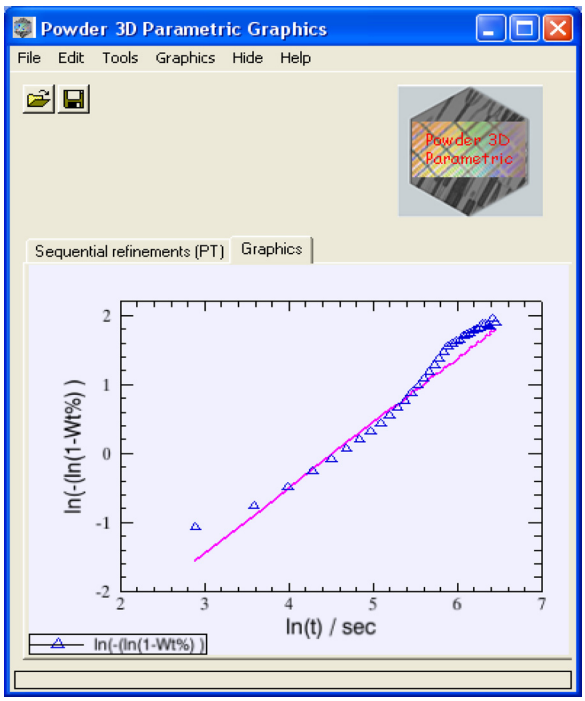

Figure 4. (Color online) The (linearized) sequentially refined weight fractions of the emerging β-Cu*PC* (diamonds) of the test-sample and the parametrically refined weight fractions of β-Cu*PC* (line) are plotted in the graphics interface.

The input file associated with parametric Rietveld refinement must contain one common part (same as the file used in the refinement of a single pattern) and as many "phase" parts as the number of powder patterns that will be used in the refinement. Each of these "phase" parts must contain a form of Eq. (1) or the keyword "*scale*."

The program makes use of the output file stored after the test refinement and places Eq. (1) or substitutes the keyword "*scale*" with Eq. (1) in the "phase" parts (e.g., in the phase α-Cu*PC*) of the file as many times as the numbers of patterns selected by the user. Before replacing the keyword "*scale*," Eq. (1) would be rewritten in such a way that S_α is at the left hand side and the Avrami equation is in place of the weight fraction x_α (Müller *et al.*, 2009).

The codes necessary to parameterize the weight percent with Avrami equation is thus automatically generated by the program and written in the large input file and executed in the TOPAS launch mode kernel.

After the completion of the refinement, the linearized weight fractions of the emerging phase (in this case β-Cu*PC*) obtained from sequential refinements and the weight fractions refined from the model (Avrami) will be plotted together in the main graphics interface of the program (Figure 4). The parameters n and k refined from the Avrami model will be read from output file returned by TOPAS and will be displayed in the parameters sheet.

D. Analysis

The kinetic parameters n and k of the test-data derived from the Avrami model and those determined from the sequential refinement (Müller *et al.*, 2010) are presented in Table I.

https://doi.org/10.1154/1.3662220 Published online by Cambridge University Press

TABLE I. The Avrami parameters (k, n) obtained from sequential refinements (Müller *et al*., 2010) are compared with those obtained from the parametric refinement (third column). The parameters in the fourth column are refined from the powder patterns that correspond approximately to the linear region (optimal time-segment) of the weight fraction curve [Figure 3(b)].

		Parametric refinement	
Parameters	Literature (sequential)	All 35 patterns	Linear region
n	1.04	0.895	1.07
k	0.0087	0.011	0.0095
r_wp	1.1	0.9	0.8

The overall weighted residual for the parametric fit using all 35 patterns is ~0.869. The aberrations in the parameters n and k (Table I, column 2) are minimized when the powder patterns that correspond to the linear part of the weight fraction curve alone is used in the parameterization [the two cases are compared in Figures 5(a) and 5(b)].

The slight variation of n and k (in Table I, column 4) from the expected values (in Table I, column 2) is due to the exclusion of crystallite size effects in the original refinements from literature (Müller *et al*., 2010).

The isothermal data for all the Cu*PC* polymorphs collected in various experiments (Table II) were analyzed in a similar manner with the help of the program. The comparison of the rate constants and the activation energies determined from sequential and parametric refinements and the explanations for the discrepancies between the results are presented in the following section.

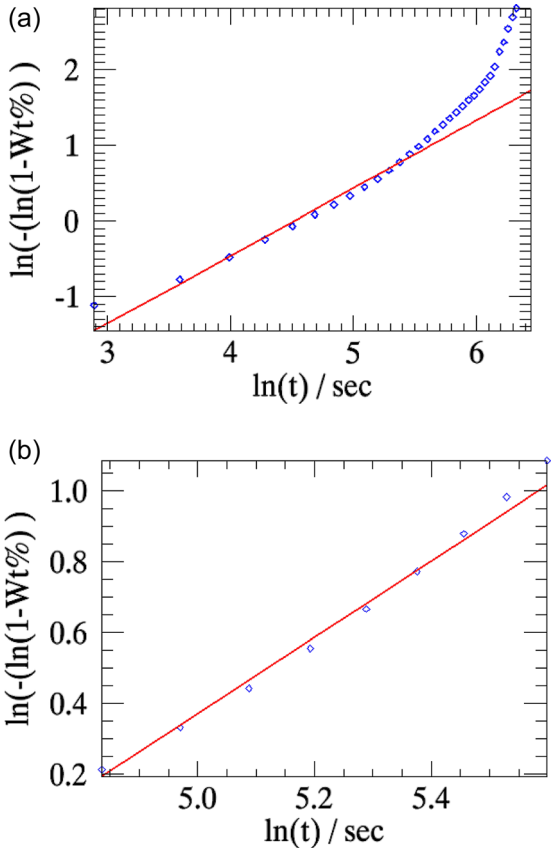

Figure 5. (Color online) The linearized weight fractions of the emerging β-Cu*PC* phase obtained in sequential refinements (squares) and in parametric refinements (line) for the test-sample are compared. (a) All 35 powder patterns are included in parameterization. (b) Only the patterns from indices 7 to 15 are used in the parameterization [Figure 3(a)].

IV. RESULTS OF PARAMETRIC RIETVELD ANALYSIS OF THE KINETICS OF COPPER PHTHALOCYANINE

Table II summarizes the reaction kinetics studies performed on several isothermal data of Cu*PC* polymorphs using sequential and parametric Rietveld refinement methods. The reaction rate constants and the activation energies obtained from parametric refinements for some selected Cu*PC* samples are individually interpreted from Sec. IV A to IV C.

A. Pure α-Cu*PC*

The kinetics of phase transition from pure α-Cu*PC* (containing no additives) to β-Cu*PC* has been studied using the time-dependent powder data collected at temperatures 230, 250, 270 and 290 °C.

1. Pure α-CuPC at 230 °C

In the experiment performed with pure α-Cu*PC* at 230 °C, a total of 348 time-dependent powder patterns were collected. Parametric Rietveld refinement could not be successfully performed for this sample when all the 348 powder patterns collected in the experiment were included in the refinement.

The weight fractions of the simultaneously decaying α-Cu*PC* and emerging β-Cu*PC* phases in this experiment performed at 230 °C as determined from sequential Rietveld refinement are plotted in Figure 6(a). As observed in Figure 6(a), the change in the weight fractions of β-Cu*PC* with respect to the experimental time is extremely low until 18 min from the beginning of experiment [approximately up to pattern number 60 (Müller *et al*., 2010)]. The stability of the refinement is strongly biased in this case, due to the inclusion of many patterns with significantly low weight fractions in the parametric refinement.

Using only the patterns recorded after the initiation of the reaction (between pattern number 60 and 348) in the parametric refinement [shown in Figure 6(b)] has resulted in its convergence and also produced a precise rate constant [comparable to the literature (Müller *et al*., 2010)]. The reliability of rate constant is maintained when the powder patterns collected after 60 min of the start of experiment alone were used in the refinement [approximately between pattern number 200 and 348, Figure 6(c)].

2. Pure α-CuPC at higher temperatures

The weight fractions of the decaying α-Cu*PC* and growing β-Cu*PC* phases in experiments performed at 250 and at 270 °C as determined from sequential refinements are plotted in Figures 7(a) and 7(b). As can be seen, pure α-Cu*PC* starts reacting faster at temperatures higher than 230 °C.

The convergence of parametric Rietveld refinements (using all the powder patterns) of pure α-Cu*PC* measured at temperature 250 °C could be easily achieved even without supplying a suitable starting value for the variable k. For this

https://doi.org/10.1154/1.3662220 Published online by Cambridge University Press

TABLE II. The reaction rate constants (k) and the activation energies (E) of the polymorphs and polymorph-additives mixtures of Cu*PC* determined from sequential (bold lettered) and parametric Rietveld refinements are presented. The temperatures at which various time-dependent experiments were performed are listed in the second column. The data measured at these temperatures are subjected to independent sequential and parametric Rietveld refinements. "Optimal" (italic letters) denotes that the rate constants and activation energies are found from parametric refinements using the powder patterns that correspond to the linear region of the weight fraction of the growing phase [Figure 3(a) and Figure 5(b)]. "-err-" indicates an unexpected error due to numerical instability during refinement. "-N.P-" sequential refinement not performed in literature (Müller *et al*., 2010). "-T.P-" indicates that two sets of parametric refinements have been performed for the sample. *DMAM*: a Cu*PC* derivative. NU: Naphthyl derivative. *BlauEFL*: the commercial form of ε-Cu*PC*.

Sample—Cu*PC*		Temperature (°C)	Avrami parameter k (rate constant) $\times 10^{-5}$			E [kJ/mol]	
			Sequential	Parametric	Optimal	Sequential	Optimal
Pure α		230	4.7	-err-	4.71	241(2)	243.1
		250	41.0	42.4	43.5		
		270	255	353	356.00		
		290	2100	-err-	2260		
90% α + 10% β		250	178	229	215.6	187(6)	175.2
		270	870	1100	950		
ε		320	0.026	0.016	0.0264	2263(9)	2302
		340	83000	108900	108253		
ε + *BlauEFL*		320	0.008	38.8	0.0069	1807(26)	2285
		330	3.40	3.9	14.97		
90%ε + 10%β	0-16%	250	6.714	-T.P.-	5.134	325(5)	34.9
	0–16%	270	95	-T.P.-	6.9		
	>16%	250	0.0721	-T.P.-	2.247	-N.P.-	58.9
	>16%	270	0.0091	-T.P.-	3.7		
90% α + 10% ε		250	447	-err.-	314.34	213(6)	233
		270	2700	-err.-	2272.63		
85.5% α + 9.5% ε + 5% *NU*		230	297	105.65	141.3	205(13)	225
		250	1926	621.95	1108.3		
85.5% α + 9.5% ε + 5% *DMAM*		230	8.7	-err-	7.85		
		250	377	48.36	243.15	413(5)	375

data, even the use of fewer powder patterns in the refinement, provided they correspond to the linear region of the weighted residual curve [Figure 7(c)], could produce precise values of the variables k and n [consistent with the literature (Müller *et al*., 2010)].

The weight fractions of β-Cu*PC* obtained in the two cases (at 250 °C) are compared with the linearized weight fractions determined from sequential refinements in Figure 8. The overall weighted residual in the parametric refinement involving the powder patterns that correspond to the linear region of the weighted residual curve is slightly lower (∼0.94) than that obtained when all the 224 patterns collected in the experiment are used in the refinement (∼1.01).

For the same sample measured at 270 °C, the linearized weight fractions of the emerging β-Cu*PC* determined using sequential refinements and the weight fractions derived from parametric refinement are plotted in Figure 9.

The rate constants k derived from the Avrami model, in all the experiments involving the transformation of pure α-Cu*PC* (from temperatures 230 to 290 °C) to β-Cu*PC* are plotted as an Arrhenius type of plot (Iordanova *et al*., 2002) in Figure 10. The slope of the regression line fitted to these rate constants gives the activation energy of the reaction (for pure α-Cu*PC*, the activation energy is ∼243 kJ/mol).

B. α-Cu*PC* and β-Cu*PC*

The kinetics of transformation of the mixture containing α and β phases of Cu*PC* in the ratio 9:1 to β-Cu*PC* was studied from their time-resolved data collected at temperatures of 250 and 270 °C. The weight fractions of the emerging β-Cu*PC* determined from parametric refinements for one of these experiments (performed at 250 °C) is plotted in Figure 11. The weight fractions of the same mixture measured at 270 °C are plotted in Figures 5(a) and 5(b).

As inferred from Table II, the addition of β-Cu*PC* to pure α-Cu*PC* has increased the rate constant k of the experiments performed at 250 and 270 °C by a factor of about 3. The activation energy of this reaction, derived from the parameterized rate constants, is about 175 kJ/ mol, which is about 70 kJ/mol smaller than the energy of the reactions involving pure α-Cu*PC*.

C. α-Cu*PC* and ε-Cu*PC* and additives

1. α-CuPC and ε-CuPC

The kinetics of phase transition of α-Cu*PC* + ε-Cu*PC* mixture (in the ratio 9:1) to β-Cu*PC* was studied from their time-resolved data collected at temperatures 250 and 270 °C. The weight fractions of the three phases involved in these experiments, determined from sequential refinements, are plotted in Figure 12.

Parametric refinement of α-Cu*PC* + ε-Cu*PC* mixture could be performed only for the data collected at the temperature 250 °C. For this data, the powder patterns that correspond to the linear region alone were used in this refinement (patterns 12–50 out of 184). The weight fractions of β-Cu*PC* derived from parametric refinement are compared

https://doi.org/10.1154/1.3662220 Published online by Cambridge University Press

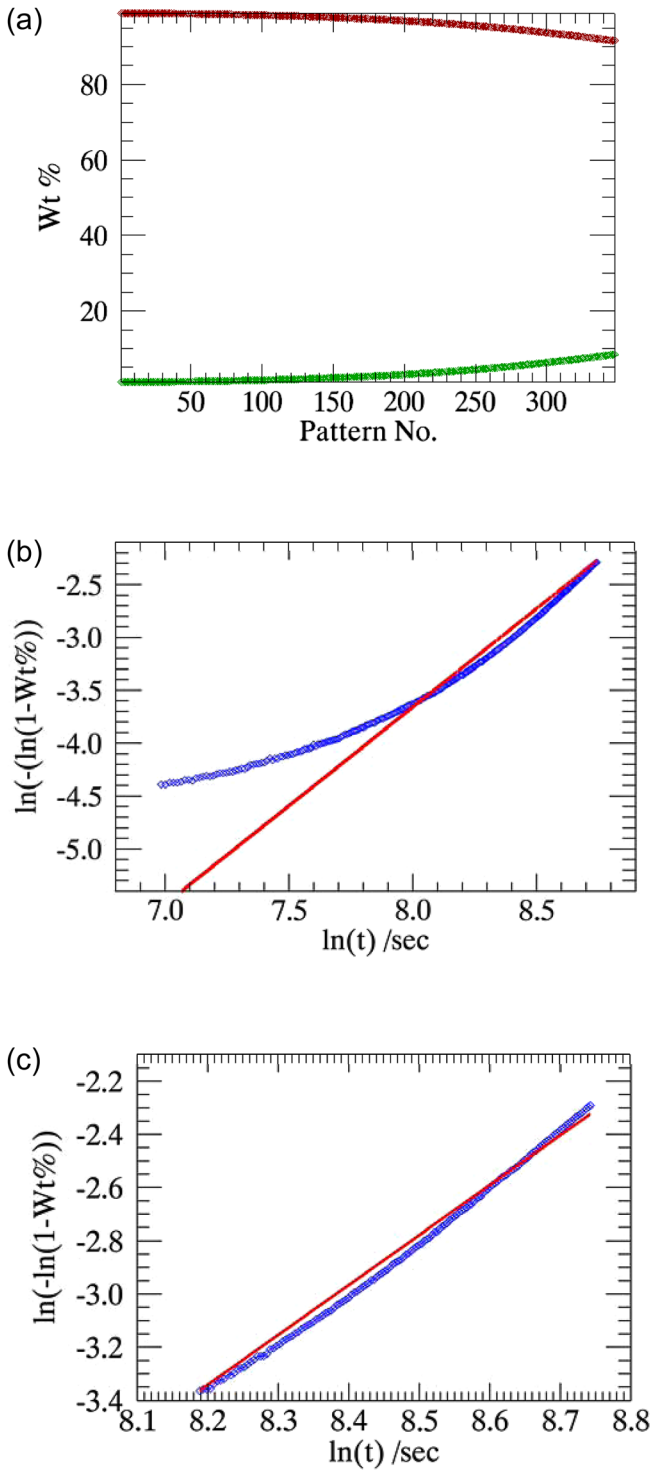

Figure 6. (Color online) (a) Weight fractions of the simultaneously decaying α-Cu*PC* and the emerging β-Cu*PC* at 230 °C, determined from sequential refinements. (b) and (c) Weight fractions of β-Cu*PC* determined from sequential refinements (squares) compared with the weight fractions determined from parametric refinements (lines). (b)The powder patterns collected after 18 min from the beginning of the experiment are used in the refinement (pattern numbers 60 to 300). (c) The powder patterns collected 60 min after the beginning of the experiment are used in the refinement (pattern numbers 200 to 300).

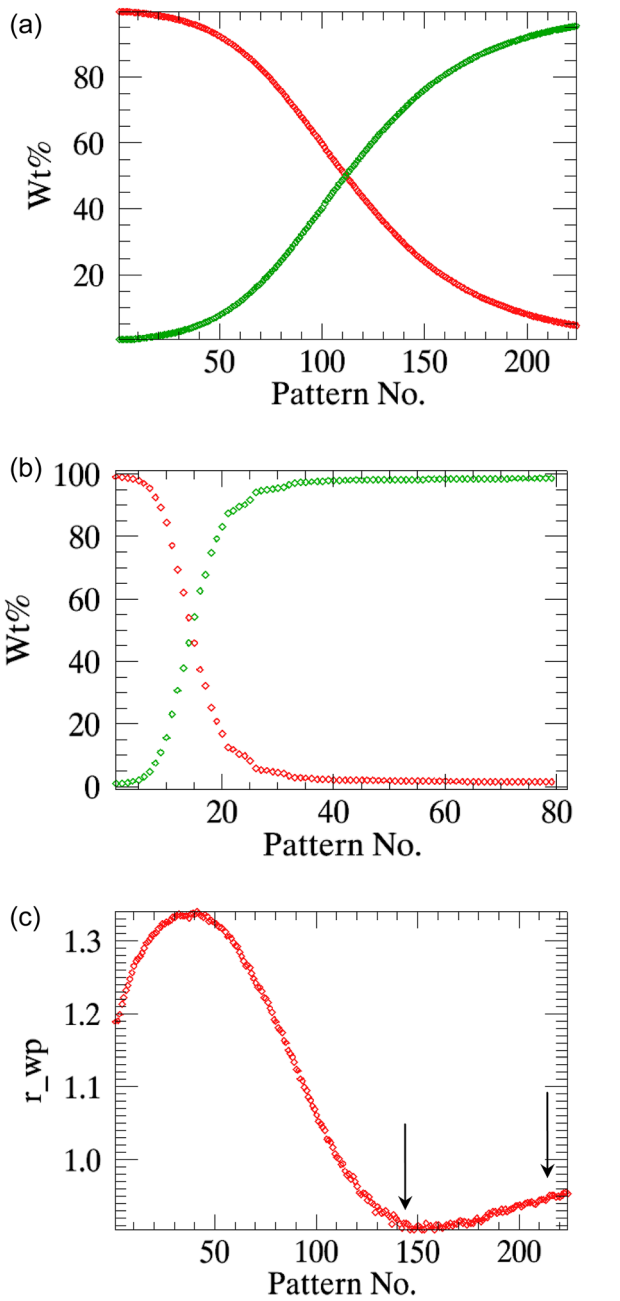

Figure 7. (Color online) Weight fractions of the decaying α-Cu*PC* and the emerging β-Cu*PC* at 250 and 270 C determined from sequential refinements are plotted in (a) and (b). Weighted residuals of the sequential refinements of pure α-Cu*PC* data measured at 250 °C are plotted in (c). The linear part of the residual curve is marked with arrows.

with the linearized weight fractions obtained in sequential refinements (Figure 13).

For the data collected at the temperature 270 °C, parametric refinement ended up in a huge standard deviation [compared to the literature (Müller *et al*., 2010)], even after using the powder patterns that belong to the linear region and supplying sensible starting values for the variables *k* and *n*. The α-Cu*PC* present in the α-ε mixture was completely transformed into β-Cu*PC* in approximately 3.6 min from the beginning of the experiment [Figure 12(b)]. The high reactivity of the α-Cu*PC* + ε-Cu*PC* mixture at 270 °C has strongly influenced the convergence of parametric refinement and also the precision of activation energy of the reaction determined using the Avrami model (∼233 kJ/mol).

The success of parametric refinement for the transformations involving ε-Cu*PC* and *BlauEFL* and also the other

https://doi.org/10.1154/1.3662220 Published online by Cambridge University Press

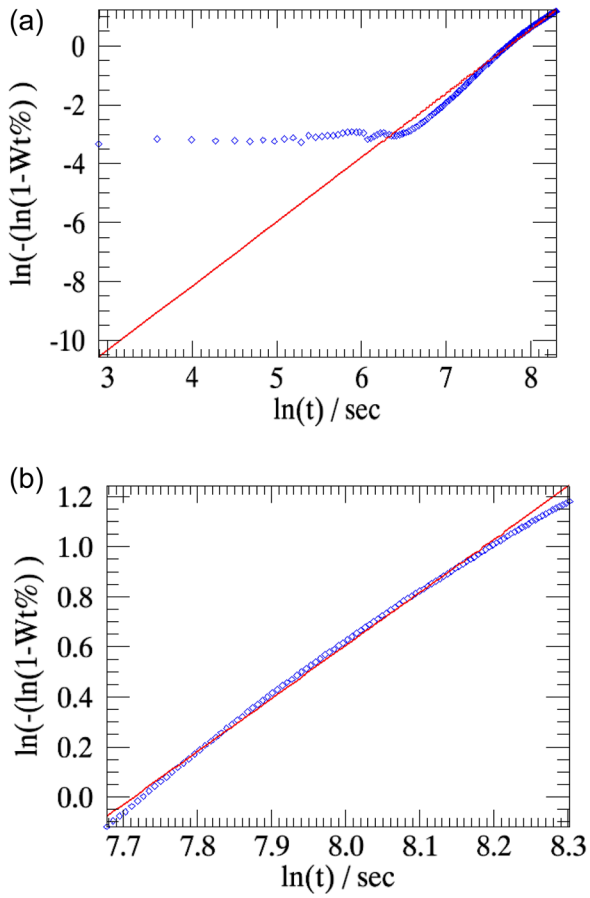

Figure 8. (Color online) The linearized weight fractions of β-Cu*PC* in the transformation from pure α-Cu*PC* to β-Cu*PC* at 250 °C from sequential refinements (diamonds) are compared to those obtained from parametric refinements (lines). (a) All the 224 powder patterns collected in the experiment are used in the parametric refinement. (b) The powder patterns that correspond to the linear region of the weighted residual curve [Figure 7(c)] alone are used in the refinement.

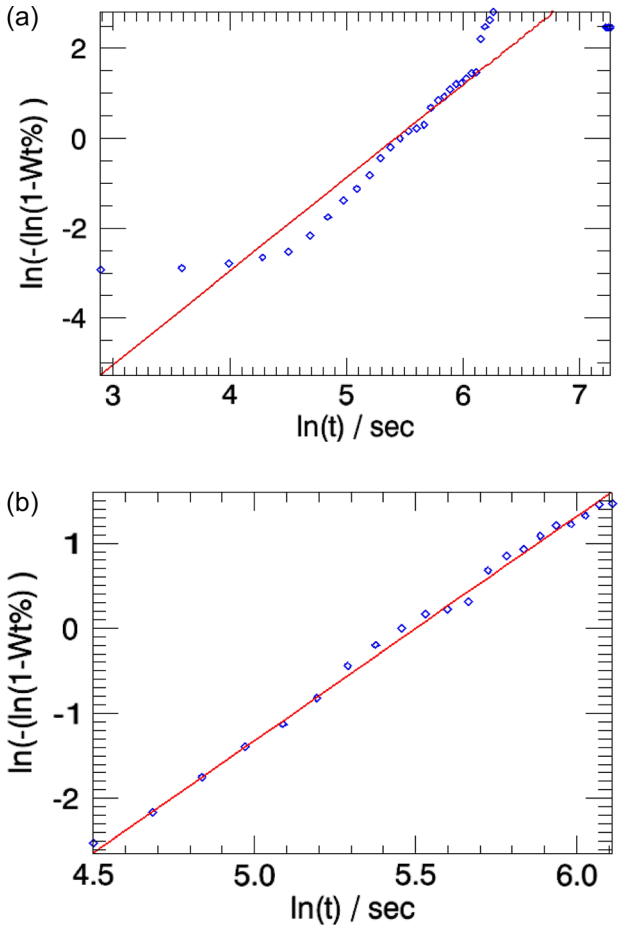

Figure 9. (Color online) The linearized weight fractions of β-Cu*PC* in the transformation from pure α-Cu*PC* to β-Cu*PC* at 270 °C, in sequential (diamonds) and parametric refinements (lines) are plotted. (a) All the 79 powder patterns collected in the experiment are used in the parametric refinement. (b) The powder patterns that correspond to the linear region of the weighted residual curve (pattern numbers 5–25) alone are used in the refinement.

measurements involving the transition of most ε-Cu*PC* samples with additives and the reaction involving three phases of Cu*PC* (e.g., α-Cu*PC* + ε-Cu*PC* to β-Cu*PC*) depended strongly on the physical sensibility of the starting value of the rate constant (k). In most of these cases (dependent on the reaction order), the starting value for the parameter k was approximated from the half-life decay equation of a first order reaction. For other samples, the coefficients obtained in the least squares fit to the linearized weight fraction were used as the starting values.

V. PARAMETERIZATION OF MICROSTRUCTURAL INFORMATION: CRYSTALLITE SIZE VARIATION WITH TEMPERATURE

In this section, a general procedure to parameterize the crystallite size variation with respect to the temperature is presented. The nanocrystalline titanium dioxide (TiO_2)-anatase data measured in dependence on temperature are used as examples. This application is considered a case study to prove that the parameterization of the crystallite size (inversely proportional to the FWHM of the phase peaks) versus time/temperature is feasible.

All the input files required for this analysis were prepared with the help of the program "POWDER 3D PARAMETRIC" (Sec. III).

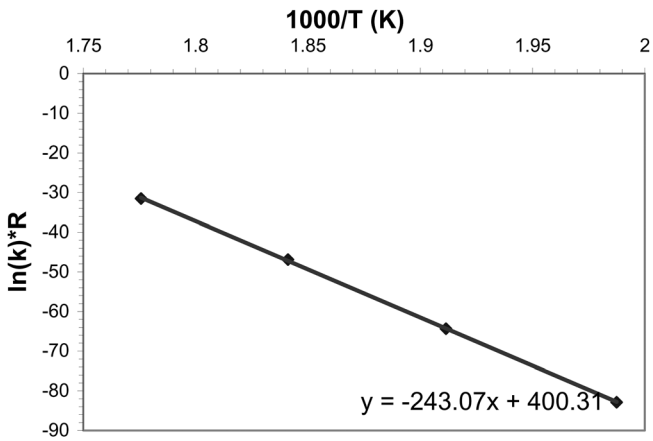

Figure 10. The rate constants of the reaction involving the transformation from pure α-Cu*PC* to β-Cu*PC* as derived from Avrami equation are plotted as an Arrhenius type plot. Linear fit has been made to these points. The slope of the regression line gives the activation energy of the reaction.

https://doi.org/10.1154/1.3662220 Published online by Cambridge University Press

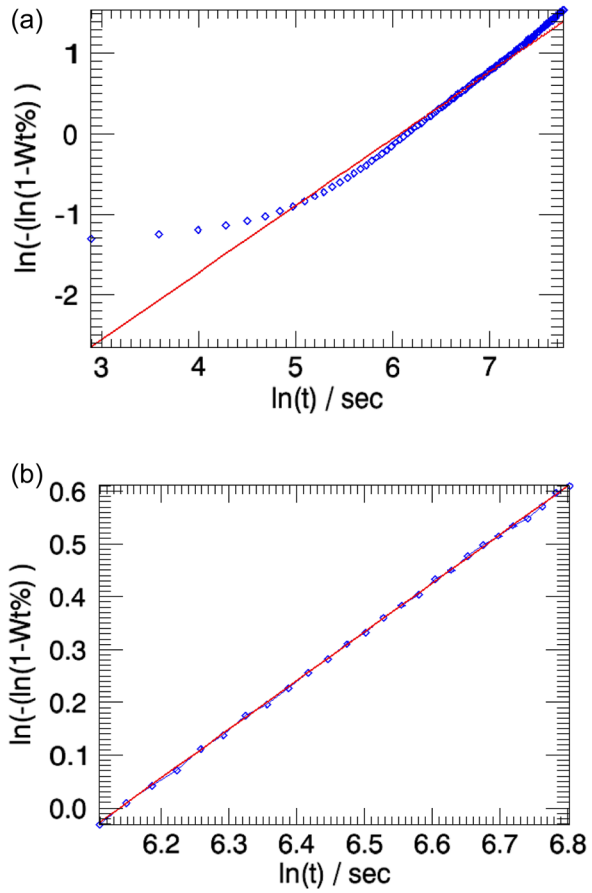

Figure 11. (Color online) The linearized weight fractions of β-Cu*PC* in the transformation of α-Cu*PC* + β-Cu*PC* mixture at 270 °C, from sequential (diamonds) parametric refinements (lines) are shown. (a) All the 130 powder patterns collected in the experiment are used in the parametric refinement. (b) Only the powder patterns that correspond to the linear region of the weighted residual curve (~pattern numbers 25–50) alone are used in the refinement.

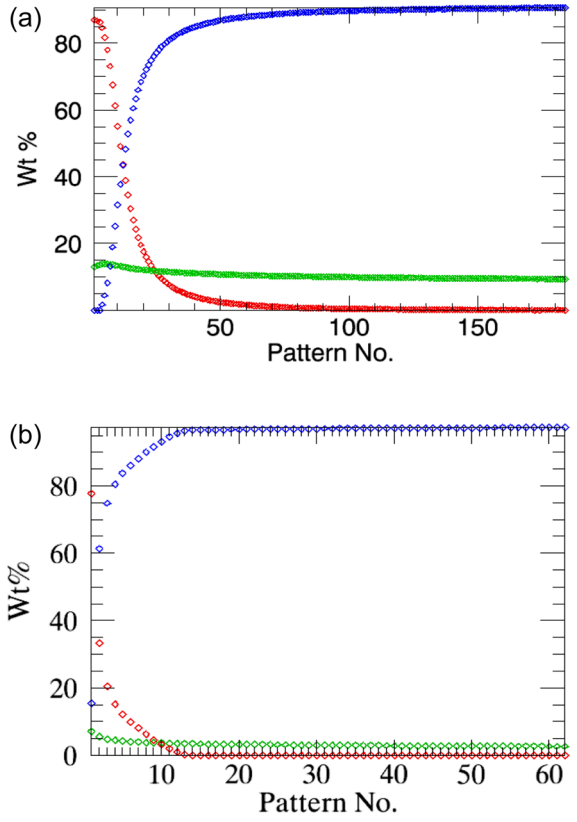

Figure 12. (Color online) The weight fractions of the decaying α-Cu*PC* and the emerging β-Cu*PC* and ε-Cu*PC* (very low and almost not changing) at 250 and 270 °C determined from sequential refinements are plotted in (a) and (b).

A. Crystallite size

The major sources of peak broadening in XRPD are the microstructure of the material (crystallite size and lattice strain) and the instrumental aberrations. In Rietveld analysis, the instrumental contributions to the peak broadening are handled by various physical and mathematical models. Once, the Caglioti relation was mainly used for this purpose (Caglioti *et al*., 1958; David *et al*., 2010).

The angle dependent (θ_k) X-ray powder peak broadening due to crystallite size can be modeled best by functions that are convolutions of Gaussian and Lorentzian functions (Coelho, 2007; Balzar *et al*., 1999). In a similar way, the lattice strain contribution to X-ray powder peak broadening can be modeled by convoluting the Gaussian and Lorentzian functions.

Altogether, the microstructural contribution to X-ray peak broadening can be satisfactorily explained by a set of four equations that are dependent on one another

$$(\beta_{sz})_{gauss} = \frac{\lambda}{S_{gauss}\cos(\theta_k)}, \tag{2a}$$

$$(\beta_{sr})_{gauss} = 4\varepsilon_{gauss}\tan(\theta_k), \tag{2b}$$

$$(\beta_{sz})_{lor} = \frac{\lambda}{S_{lor}\cos(\theta_k)}, \tag{3a}$$

$$(\beta_{sr})_{lor} = 4\varepsilon_{lor}\tan(\theta_k), \tag{3b}$$

where $(\beta_{sz})_{gauss}$ and $(\beta_{sz})_{lor}$ are the Gaussian and Lorentzian related FWHM of the size broadened phase peak, $(\beta_{sr})_{gauss}$ and $(\beta_{sr})_{lor}$ are the Gaussian and Lorentzian related FWHM of the strain broadened phase peak. $(S)_{gauss}$ and $(S)_{lor}$ are the Gaussian and Lorentzian related crystallite size of the

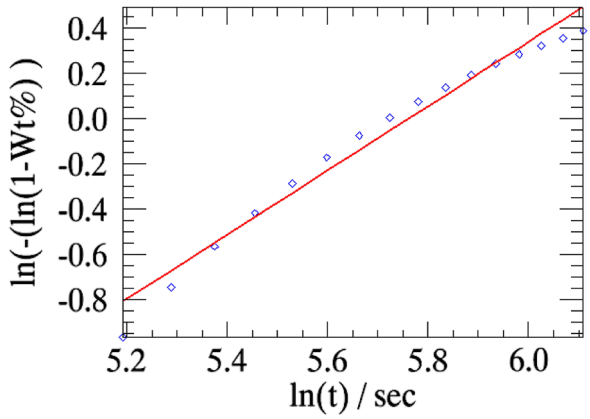

Figure 13. (Color online) The weight fractions of β-Cu*PC* in reaction involving the transformation of α-ε-mixture of Cu*PC* to β-Cu*PC* at 250 °C from parametric refinement (line) are compared with the linearized weight fractions of β-Cu*PC* determined from sequential refinements (diamonds). Only 38 out of 184 powder patterns were used in the parametric refinement.

https://doi.org/10.1154/1.3662220 Published online by Cambridge University Press

material. $(\varepsilon)_{gauss}$ and $(\varepsilon)_{lor}$ are the Gaussian and Lorentzian related lattice strain of the material. λ is the wavelength of the incident X-ray beam, and θ_k are the phase peak positions.

Depending upon the necessity, some of these equations can be introduced as microstructural convolution models of the material during the Rietveld refinement.

TOPAS launch mode offers a simple way to introduce these models [Eqs. (2a)–(3b)] during the Rietveld refinement using its built-in macros *CS_G*, *CS_L*, *Strain_G*, and *Size_G*. These macros can be introduced into the input file to directly refine the Gaussian and/or Lorentzian related crystallite size (or lattice strain) of the material.

Parameterization of one of these equations with respect to time/temperature can be easily accomplished by modifying and rewriting the contents of these macros in the prepared "parametric input file." For instance, the parameterization of Gaussian related crystallite size versus time-temperature with a quadratic equation [Eq. (4)] can be accomplished by replacing the respective FWHM [Eq. 2(a)] by the model equation and rewriting the size term (S_{gauss}) and the FWHM term $(\beta_{sz})_{gauss}$, as in Eq. (5)

$$y = (a_0 + a_1 T + a_2 T^2), \tag{4}$$

$$S_{gauss} = \frac{\lambda}{(a_0 + a_1 T + a_2 T^2)\cos(\theta_k)}, \tag{5}$$

where y is the dependent variable, a_0, a_1, a_2 are the refinable (global) model coefficients, and T is the experimental temperature (or other external variable).

The coefficients of the quadratic function (a_0, a_1, and a_2) are refined from multiple powder patterns collected in the experiment; therefore, these variables must be defined in the common part of the "parametric input file" (Sec. III C).

Equation (6) gives the TOPAS macro language statements analogous to Eqs. (4) and (5). These statements will be automatically generated by the program and written in the appropriate locations in the "phase" parts of the "parametric input file" before its execution (as explained in Sec. III C)

```
gauss_fwhm = (a0 + a1*T_298 + a2*T_298^2
           + a3*T_298^3);
local fwhm_1 = Get (gauss_fwhm);
local siz1 = 0.1 Rad(Lam)/(cos(Th)(fwhm_1));    (6)
```

where T_298 represents the experimental temperature (298 K), fwhm_1 is the Gaussian related FWHM, and siz1 is the Gaussian related crystallite size. The keywords "Get," "Lam," "gauss_fwhm," "Th" are the reserved TOPAS keywords and macros.

A simple example of parameterization of the Gaussian related crystallite size versus temperature [performed using equations analogous to Eq. (6)] is explained in the following section.

B. Gaussian crystallite size of TiO_2-anatase

The phase transition of the nanocrystalline TiO_2 from its anatase to rutile form was studied using *in situ* XRPD patterns collected at a synchrotron source. In total, 90 powder diffraction patterns in dependence on temperature were collected for this analysis (from 298 to 1123 K, with a heating rate of 6.875 K/min).

The anatase to rutile transition occurs approximately at a temperature of 700 K (Figure 14). Full quantitative sequential Rietveld analysis was performed individually and sequentially on all the patterns (for the two phases) collected in the experiment.

The Gaussian-crystallite sizes of the phase peaks of TiO_2-anatase, determined from the sequential refinements, are plotted in Figure 15. As an initial attempt, cubic function was used to model the Gaussian-crystallite size variation with temperature. The Gaussian-crystallite sizes derived from the cubic model are compared with those determined from sequential refinements in Figure 15.

As observed from Figure 15, the cubic function was unable to completely describe the variation of crystallite size versus temperature. In particular, the deviation of the fit is significantly higher in the lower temperature region (roughly from experimental temperature 298 to 409 K).

The crystallite size curve was therefore divided into two different growth regions; the patterns that belong to the two regions are independently parameterized with two different functions.

The crystallite size of TiO_2-anatase remains approximately constant from room temperature up to 409 K. This region was parameterized with a linear function. The region from 418 to 659 K that corresponds to the growing stage of TiO_2-anatase phase was modeled by a cubic function. The parametrically derived crystallite sizes of both temperature regions are plotted in Figure 16; the model coefficients obtained in the two independent parametric refinements are summarized in Table III.

The relatively smooth high temperature region (from temperatures 418 to 659 K) of the crystallite size curve could be conveniently parameterized by a cubic function. The parameterization of the low temperature region (298–409 K) with the linear model resulted in coefficients

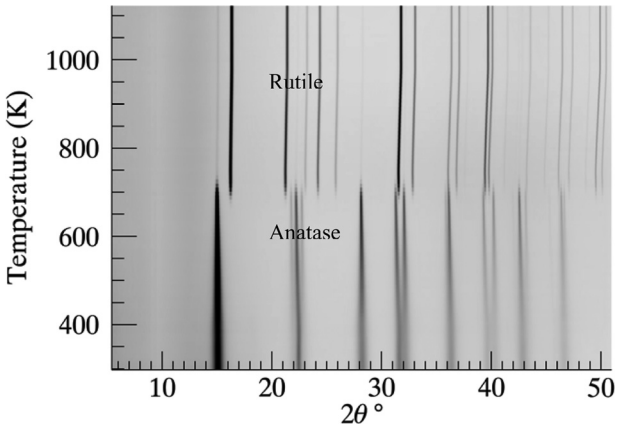

Figure 14. The anatase to rutile phase transformation of TiO_2 is shown as a simulated "heating Guinier film plot." The phase transition occurs approximately at the temperature 700 K.

https://doi.org/10.1154/1.3662220 Published online by Cambridge University Press

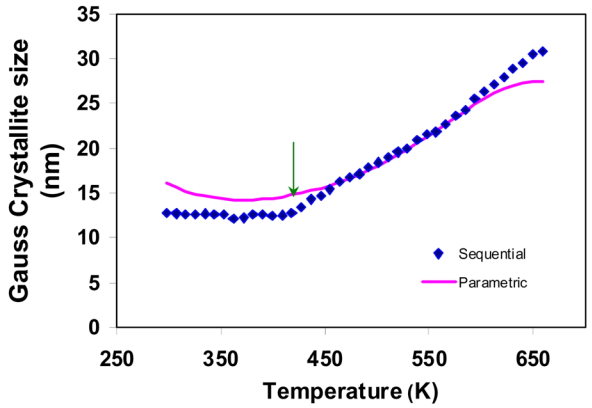

Figure 15. (Color online) The Gaussian-crystallite size of TiO_2-anatase obtained in sequential refinements (diamonds) and parametric refinements (curve) using cubic model are compared.

with lower statistical significance, as the growth of the crystallite in this temperature region is nonuniform and also the growth rate is negligibly small.

Surface effects might be considered as a reason for the inhibited growth of the crystallites in the low temperature region (298–409 K).

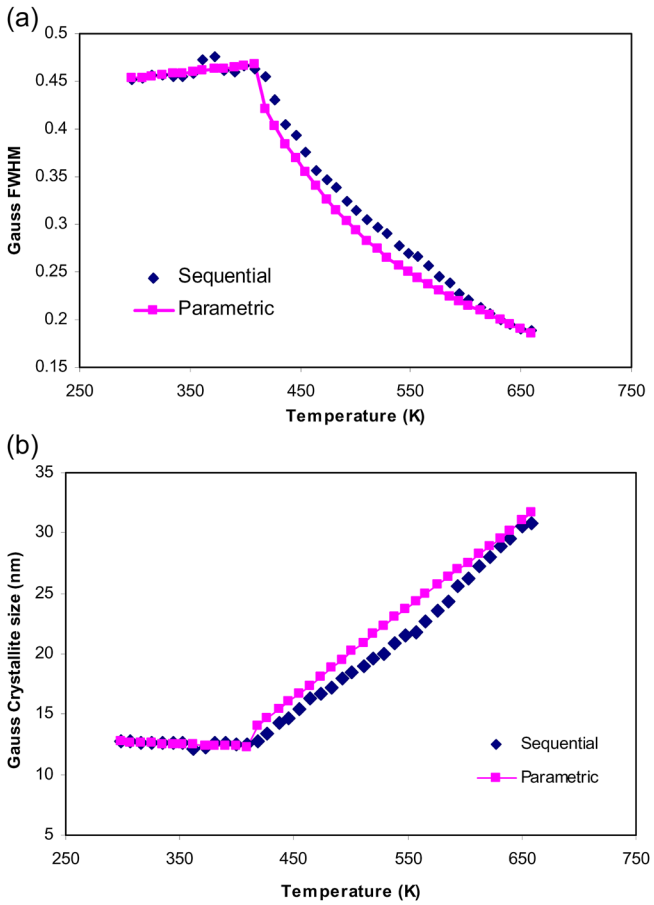

Figure 16. (Color online) The Gaussian related FWHM (top) and Gaussian-crystallite size (bottom) of TiO_2-anatase obtained in sequential refinements (diamonds) and parametric refinements (squares & lines) using cubic model are compared.

TABLE III. The coefficients of the linear and cubic functions obtained in the independent parametric refinements of two growth regions of TiO_2-anatase are presented.

Temperature range (K)	Model	a_0	a_1	a_2	a_3
298–409	Linear	0.4136	0.00013133	—	—
418–659	Cubic	3.2697	−0.0134195	0.00002011	−0.000000011

VI. SUMMARY

Parametric Rietveld refinement is an alternative and robust WPPF approach that opens the possibility to simultaneously refine multiple powder patterns collected in 2D XRPD experiments and thus allows for the introduction of variable models (or constraints), as a function of external variables, into the refinement. The program "POWDER 3D PARAMETRIC" described in this paper provides a simple way to perform both parametric and fast sequential refinements of a large number of powder patterns. The use of the program in the two applications has considerably eased the entire sequential/parametric analysis of bulk 2D XRPD data, which would otherwise demand a huge amount of manual effort and prove very time consuming. In total, about 2700 powder patterns in relation to the two applications were successfully evaluated using sequential/parametric refinement methods, assisted by the program. Except for the test refinements, the TOPAS input files required for all other refinements were automatically prepared by the program.

The program also offered a convenient and a quicker way to analyze the data measured between specific time-temperature steps. Many Cu*PC* data used in this analysis also demanded that only certain part of the data to be used in parametric refinement.

On the whole, kinetic analysis of Cu*PC* using parametric refinement could be successfully performed for most Cu*PC* data samples, except that the stability of refinements for many data samples showed dependence on the reactivity of the polymorphs. The activation energies determined for from Avrami's relation for various reactions characterize the difference in nucleation and crystallite growth processes of the related polymorph. Significant improvements in activation energies can be achieved by performing more experiments at different temperatures.

In the second application, the feasibility of parameterization of microstructural variables (Gaussian-crystallite size) has been verified using the temperature dependent TiO_2 data. The input files required for several trials of parametric refinements with various crystallite size models and various time segments were prepared quickly and conveniently using the options provided by the program [(Figures 2(b)]. The variation of Gaussian-crystallite size versus temperature for the growth region of TiO_2-anatase could be successfully parameterized with a higher order polynomial; however, the convergences of these refinements demanded physically sensible starting values for the model coefficients. In most trials, the convergence of parametric refinement showed strong dependence on the smoothness of

https://doi.org/10.1154/1.3662220 Published online by Cambridge University Press

variation of the crystallite size with respect to temperature and on the quality of the data.

The parameterization of microstructural variables with temperature as introduced in this paper is a basic application. As such, it can be used only to stabilize other refinable variables during parametric refinement, provided that the model used is appropriate.

ACKNOWLEDGMENTS

We acknowledge our colleague Dipl. Min. Melanie Müller for performing the time-dependent measurements with Cu*PC* and also for helping us in preparing the TOPAS input file required for the "test" refinements. Our former colleague Dr. Stefan Ghedia is gratefully acknowledged for carefully proofreading the article.

Avrami, M. (**1939**). "Kinetics of phase change I. General theory," J. Chem. Phys. **7**, 1103–1112.

Avrami, M. (**1941**). "Granulation, phase change, and microstructure kinetics of phase change. III," J. Chem. Phys. **9**, 177–184.

Balzar, D. (**1999**). "Voigt-function model in diffraction line-broadening analysis in defect and microstructure analysis from diffraction," International Union of Crystallography Monographs on Crystallography No. 10 (Oxford University Press, New York).

Caglioti, G., Paoletti, A., and Ricci, F. P. (**1958**). "Choice of collimators for a crystal spectrometer for neutron diffraction," Nucl. Instrum. **3**, 223–228.

Coelho, A. A. (**2007**). TOPAS, v4.0, Bruker AXS, Coelho 2007 (Brisbane, Australia).

David, W. I. F., Leoni, M., and Scardi, P. (**2010**). "Domain size analysis in the Rietveld method," Mater. Sci. Forum **651**, 187–200.

Farjas, J. and Roura, P. (**2006**). "Modification of the Kolmogorov-Johnson-Mehl-Avrami rate equation for non-isothermal experiments and its analytical solution," Acta Mater. **54**, 5573–5579.

Hill, R. J. and Howard, C. J. (**1987**). "Quantitative phase analysis from neutron powder diffraction data using the Rietveld method," J. Appl. Crystallogr. **20**, 467–474.

Hinrichsen, B., Dinnebier, R. E., and Jansen, M. (**2006**). "Powder 3D: An easy to use program for data reduction and graphical presentation of large numbers of powder diffraction patterns," Z. Krist. **23**, 231–236.

Iordanova, R., Lefterova, E., Uzunuv, I., Dimitriev, Y., and Klissurski, D. (**2002**), "Nonisothermal crystallisation kinetics of V_2O_5-MoO_3-Bi_2O_3 glasses," J. Therm. Anal. Calorim. **70**, 393–404.

Malek, J. and Mitsuhashi, T. (**2000**). "Testing method for the Johnson-Mehl-Avrami Equation in kinetic analysis of crystallization processes," J. Am. Ceram. Soc. **83**, 2103–2105.

Müller, M., Dinnebier, R. E., Jansen, M., Wiedemann, S., and Plueg, C. (**2010**). "The influence of temperature, additives and polymorphic form on the kinetics of the phase transformations of copper phthalocyanine," Dyes Pigm. **85**, 152–161.

Müller, M., Dinnebier, R. E., Jansen, M., Wiedemann, S., and Plüg, C. (**2009**). "Kinetic analysis of the phase transformation from α to β-copper phthalocyanine: A case study for sequential and parametric Rietveld refinements," Powder Diffr. **24**, 191–199.

Rajiv, P., Dinnebier, R. E., and Jansen, M. (**2010**). "POWDER 3D PARAMETRIC—A program for automated sequential and parametric Rietveld refinement using TOPAS," Mater. Sci. Forum **651**, 97–104.

Stinton, G. W. and Evans, J. S. O. (**2007**). "Parametric Rietveld refinement," J. Appl. Crystallogr. **40**, 87–95.